SLAC–PUB–5843
June 1992
(N)

IR Mechanical Design for B Factories

Gordon Bowden

Stanford Linear Accelerator Center. Stanford, CA 94305 USA

ABSTRACT

Bringing e^+e^- beams of unequal energy to collision inside a detector for the study of B mesons presents new problems of mechanical support, alignment, magnet design and vacuum engineering.

1. INTRODUCTION

In past storage ring experiments, the design of the physics detector has been largely separate from the design of accelerator hardware. Detector design would start after machine design and was built around it. For several reasons this is no longer practical for the IR region of an asymmetric B factory. Physics objectives pose 3 groups of engineering problems in the IR region:

1. Energy asymmetry (3 GeV e^+/9 GeV e^-) requires merger of 2 separate storage rings at the IR.
2. High luminosity (3×10^{33}), 15 times previous rings requires extreme low β optics with focusing magnets located inside the detector. Very large average beam currents of $1.5 - 3.0$ amps generate synchrotron light, beam image currents and HOM heating inside the detector.
3. Clean vertex detection of B meson decays requires a high resolution Vertex Detector built closely around the IP vacuum pipe. Low backround noise necessitates synchrotron light masks inside the detector and very good 10^{-10} vacuum in the IR region.

A B-factory IR presents new challenges in magnet design, support and alignment, vacuum and heat transfer. A new level of integration between machine and detector is required.

Work supported by Department of Energy contract DE-AC03-76SF00515.

The new generation of B-Factories is not the first time integration of detectors with a two ring machine in confined space has been undertaken.

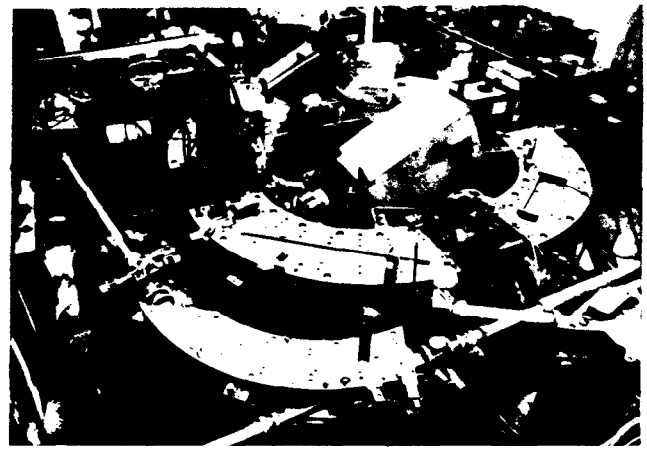

Figure 1. Princeton-Stanford 500 MeV e^-e^- storage rings, 1960.

2. BEAM MERGER

Because beams must be different in energy to separate decay vertices, they must be stored in separate rings and separately aimed at the collision point. Adjustment of magnets common to both beams close to the IP affect each independent ring differently. The fewer magnets shared in common

Contributed to The B-factories: The State of the Art in Accelerator Detectors and Physics, Stanford, CA, April 6–10, 1992

by both rings, the easier alignment and tuning will be. The very thin fan shaped beams required for high luminosity make alignment critical. Figure 2 below shows the beam envelope for the PEP II design.

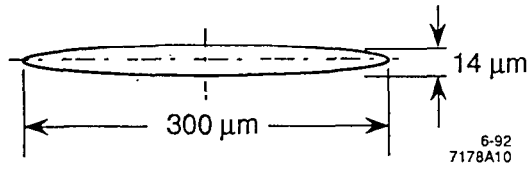

Figure 2. PEP II IP beam spot

In a two ring machine, collision is no longer guaranteed by a shared guide field for both e^+ and e^- beams. To maintain luminosity, magnets will require long term stability at the micron and milliradian level. These requirements are similar to those of the first generation linear collider SLC.

Most current B-factory designs are filled with magnetic elements around the beam merger points leaving little room for magnet coils, magnet yokes and vacuum pumps. Three IR layouts are shown below in figures 3,4,5.

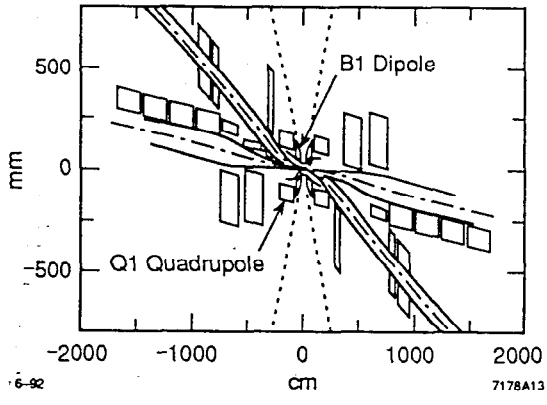

Figure 3. PEP II SLAC,LBL,LLNL

In addition to focusing magnets, other special beam optics equipment will be required in the IR region. Beams will collide either head on or at a finite angle. The head on approach requires dipole magnets to bend the converging low and high momentum beam lines onto a common head on trajectory. These dipole magnets are either placed as close to the IP as possible in the PEP II case (fig.3) or just before the last focusing lens in the HELENA case (fig.5).

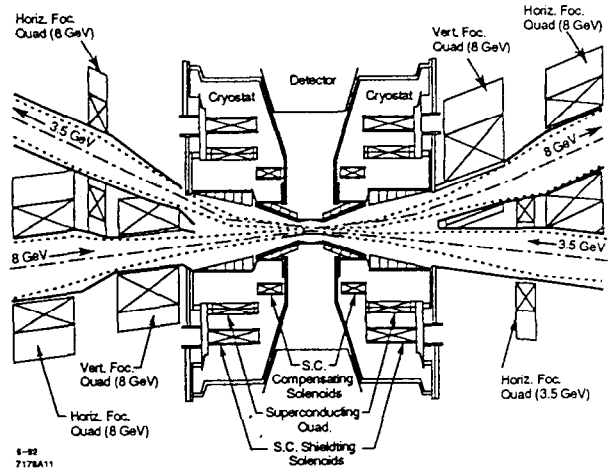

Figure 4. CESR-B Cornell

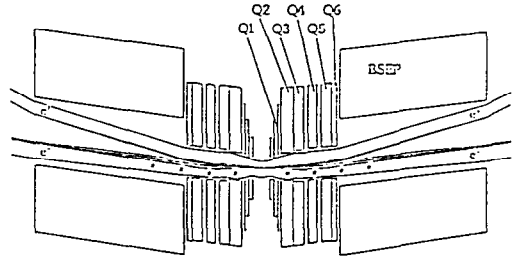

Figure 5. HELENA DESY.

To collide beams at a finite angle, bunches must have their head-tail axis rotated into alignment before collision and then realigned with their direction of motion before reentering the ring lattice. Figure 6 illustrates this so called "crab crossing".

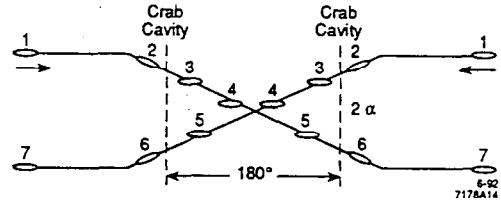

Figure 6. Crab crossing at finite angle

Crab crossing will involve rf cavities, probably superconducting, close to the collision point. Figure 6 shows the cavities located at 90° betatron phase advance from the IP. This point is generally inside the final focusing magnets. There are also

other suitable locations further out. In any case 4 phase locked cavities are needed. Making room for this equipment will have a major impact on the mechanical design of the IR region.

The usual storage ring detector has endcap doors which roll back for access to the central detector components. Direct roll back along the beam line is blocked by the many beamline components required in a high luminosity two ring machine. Figure 7 illustrates one solution where the door is split into two halves which roll straight back along angled tracks.

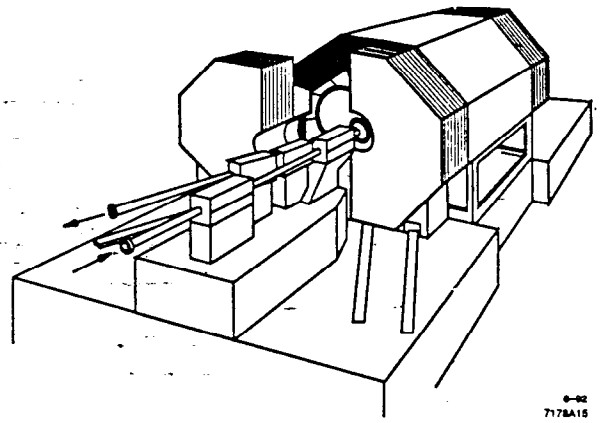

Figure 7. Detector access

In most detectors the boundary between endcap and barrel regions is a conical surface with vertex at the IP. By retracting the doors at an angle slightly less than this cone angle, clearance between the moving doors and the stationary barrel will increase as doors roll out.

3. Septum Magnets

The optics of most B-factory IR designs require a focusing quadrupole on one of the beamlines close to the point where the two beam lines merge into a common vacuum pipe. There are several magnetic designs which allow two slightly separated beamlines through the same magnet. A field free channel for the second beamline can be created by using an iron mirror plate to replace one half of the quadrupole field. Figure 8 shows the iron/coil layout for the iron mirror septum quad used just outside the detector of the CESR-B design. The iron septum separating the two beam lines can be made extremely thin at the quad center where the normal quadrupole field is zero and no flux carrying capacity is needed.

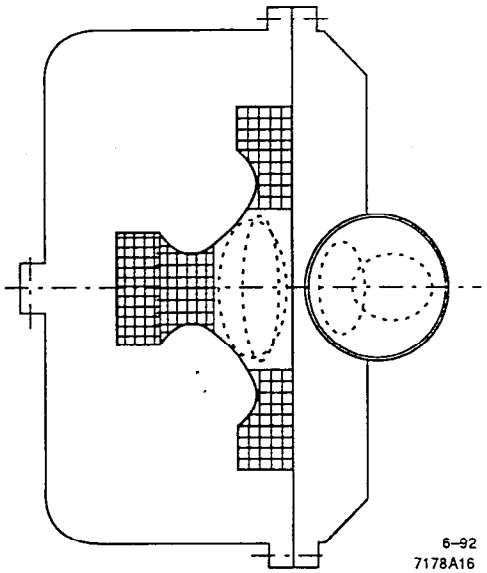

Figure 8. Iron mirror septum

Although an iron septum effectively shields the second beamline from magnetic fields, this magnet requires the first beam to be offset from the quad axis. This offset imposes an additional dipole bending field on the focused beam. If the focused beam cannot be offset from the quad's center, a current septum must be used to separate the two beam lines as shown in figure 9. In this magnet, coils on one side have been moved in from their normal iron recess to leave a field free iron shielded channel behind them for the second beam.

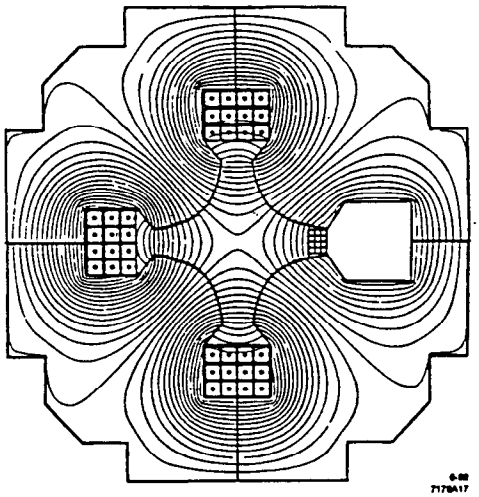

Figure 9. Current septum quad

Figure 10 shows the mechanical design of Q2 for PEP II. In this magnet, the septum portion of the coil carries a much increased current density and is cooled by 6 parallel water channels. Magnetic field just outside the septum in the low field bypass channel for the second beam falls off to about 25 gauss on beamline.

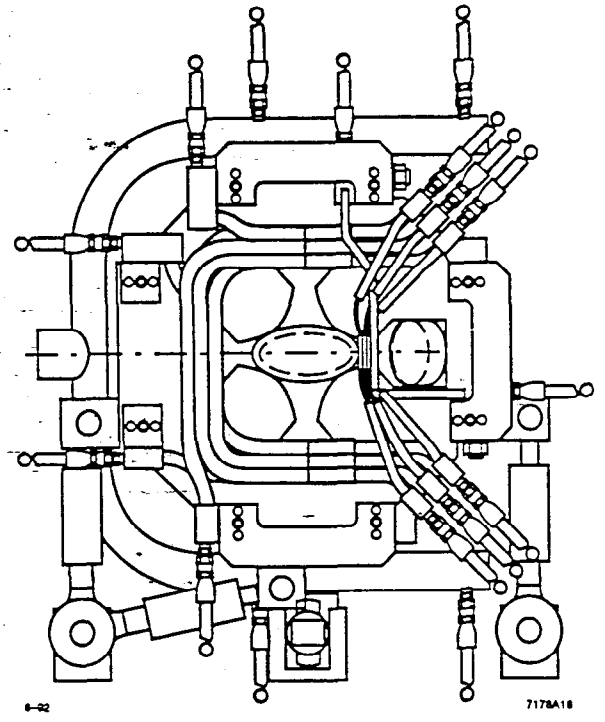

Figure 10. PEP II Q2 septum quadrupole

Pole tip inscribed radius,r_0	42.3 mm
Gradient	11.5 T/m
Length	0.5 m
Current	1367 amp
No. of turns	6
Peak field in iron pole	0.9 T
Septum current density	77 amp/mm^2
Total power	25.5 kW
Estimated weight	450 kg

Table 1. Q2 dimensions

4. Beam Heating

High beam currents needed for B-factory luminosity cause heating both by synchrotron light and a combination of beam pipe eddy current heating and Higher Order Mode heating. In the IR region most of the synchrotron light comes from off-center quads or final bend magnets such as B1 in the PEP II magnetic separation design. The pair of 2 amp beams of PEP II radiate 90 kW of synchrotron light from the IR region but most of it shines down the high energy ring beam pipe as shown in figure 11.

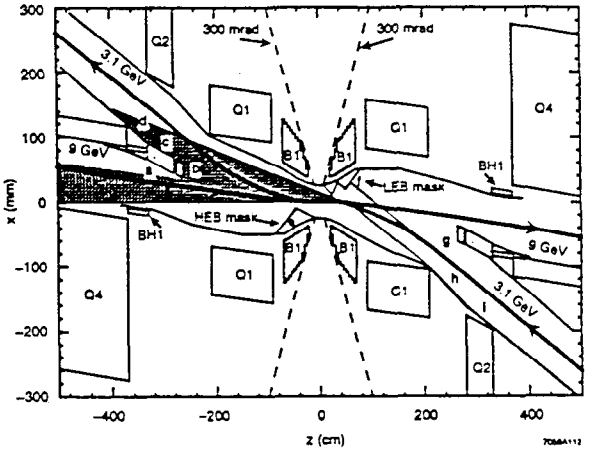

Figure 11. Low-energy beam synchrotron fans

In magnetic separation schemes such as PEP II, a small fraction of the light, mostly from the exiting bend of the low energy e^+ beam in B1, shines on the septum separating the two beam lines in Q2. This 'crotch' region must be shielded by a water cooled mask (Fig.12) which intercepts 3.7 kW of the light fan on a 2.3° grazing incidence water cooled GLIDCOP^{TM} copper mask. The maximum heat flux density on the water cooled surface is 3.5 watts/mm^2. The mechanical design of this structure must avoid any RF pickup loops, and allow accurate alignment. The vacuum pipe floor below the mask is shaped as a mirror image of the mask to form a smooth bifurcation of the beam pipe reducing beam RF HOM losses and transverse wakefields. It is perforated to allow an ion pump below to remove gas evolving from the heated mask surface .

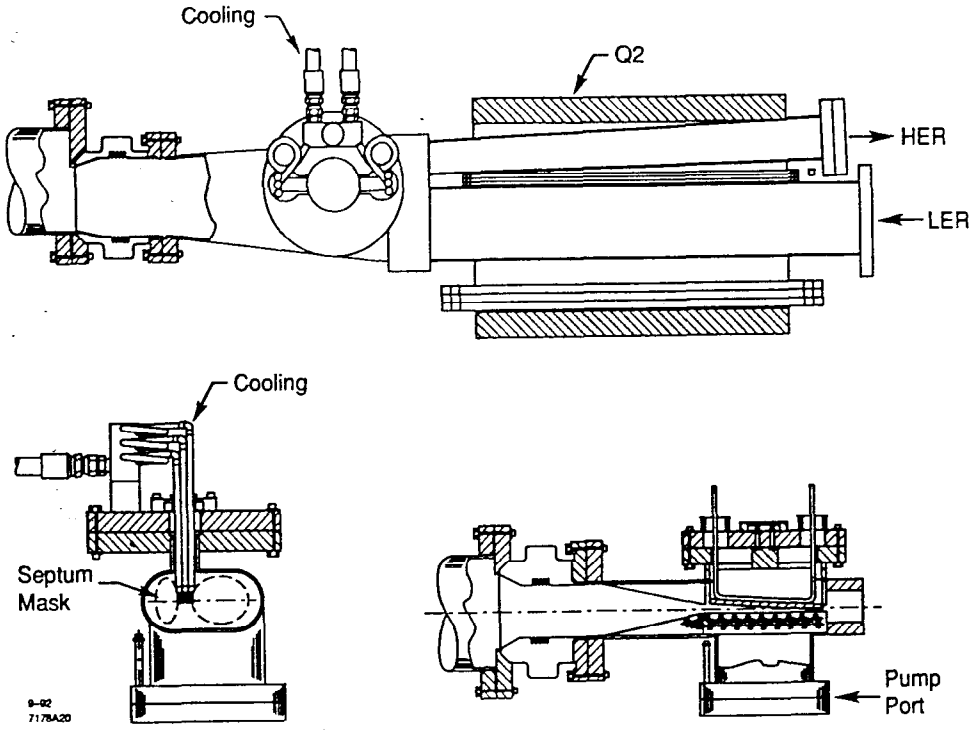

Figure 12. Septum Crotch Mask

Another source of more distributed heat is beam image current in the vacuum beam pipe wall. This power density depends on the average beam current I, the metal skin depth and is also a function of the bunch spacing and bunch length [1]. The power absorbed per unit length is:

$$\frac{P}{l} = \frac{\Gamma(3/4)}{4\pi^2 a}\frac{I^2 S_b}{\sigma_z{}^{3/2}}\sqrt{\frac{c\mu_0}{2\sigma_{dc}}} \quad \text{watts/m}$$

Here σ_{dc} is the wall electrical conductivity $(\Omega\ \text{m})^{-1}$, a the pipe radius, S_b is the inter-bunch spacing and σ_z is the bunch length. In the IP region where the current is approximately double the average ring current, $P/l \simeq 200$ watts/m for a 6 cm diameter stainless steel beam pipe. Beam pipe structures which act as RF pickup loops, whether by design or unintentionally can absorb significant power from the beam. A worst case but calculable example is a Beam Position Monitor pickup electrode. Here image currents in the wall split evenly between the electrode transmission line and the signal cable. For electrodes intercepting 1/8 of the image current, the power coupled into a matched 50 Ω line can be significant.

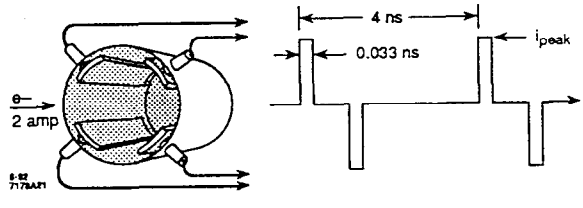

Figure 13. BPM pickup power

$$i_{peak} = \left(\frac{4\ \text{ns}}{.033\ \text{ns}}\right)\left(\frac{1}{2}\right)\left(\frac{2\ \text{amp}}{8}\right) = 15.5\ \text{amp}$$

$$P = 2\left(\frac{.033\ \text{ns}}{4\ \text{ns}}\right)(15.15\ \text{amp})^2(50\ \Omega)$$

$$P = 189.4\ \text{watts/electrode}$$

HOM losses for other geometries can be calculated [2] ,[3] or measured [4]. These heat loads generally require water cooling on all beamline components. At the interaction point where radiation thickness must be minimized, a double-walled Beryllium beam pipe with He gas cooling is used in the PEP II design (figure 14).

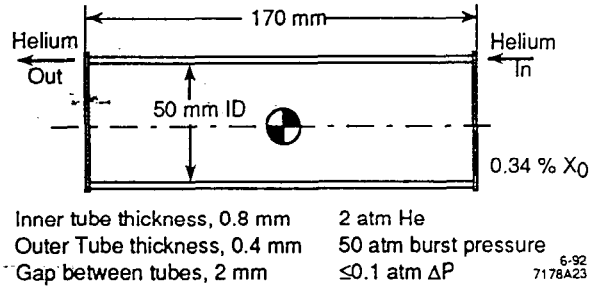

Figure 14. PEP II IP Beam Pipe

5. Internal Low β Magnets

High luminosity low β optics will require focusing magnets inside the detector. How close magnets can be brought toward the IP is limited by the detector acceptance ($\simeq$ .3 radian, 17°) and the final magnet outer radius ($\simeq$ 5 cm) to about 16 cm in the PEP II case. The minimum IP beam pipe radius is set by the need to pass the synchrotron fans from incoming beams. There are three options for putting focusing magnets inside the solenoid field of the detector.

a Conventional iron/copper coil magnets could be used if they were shielded against saturation in the detector field by a superconducting flux shield.

b A strong focusing field can also be produced by permanent magnets. If magnetization is sufficiently well fixed, as in Rare Earth Cobalt materials, external magnetic field sources will not significantly distort internal magnetization. Free of any easily permeable component, these materials have $\mu \simeq \mu_0$ and superposition of fields holds.

c Iron free superconducting magnets can be used whose field is fixed by their coil geometry.

Because of its complexity and large size, option (a) has been ignored. Both permanent magnets and superconductors have their own unique advantages. For magnetic beam separation which requires dipoles inside the detector solenoid, permanent magnets are largely free from aligning torques between their field and the solenoid because of their negligible external fringe field. On the other hand it is difficult to find space in the bore of these magnets for water cooled copper trim coils which give more than a few % of their 1 Tesla remanent field. If a finite crab crossing angle is used to collide beams, superconductors can be used with fully adjustable field strength and high gradients in large bores (up to 20 T/m and 90 mm bore in Q1 for CESR-B). One potential disadvantage of the superconductor compared to the permanent magnet in the Halbach form [5] is the effect of its fringe field on track reconstruction (figure 15). This fringe field can be largely cancelled by an additional set of outer coils at the cost of gradient loss [6].

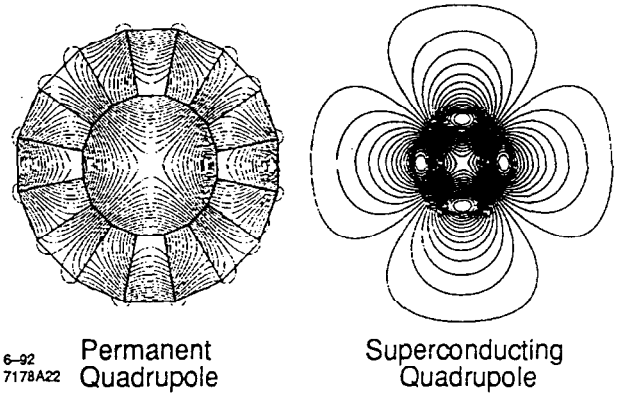

Figure 15. Quadrupole field patterns

Mechanical support of coil forces is an important and well understood aspect of superconducting magnet design. Similar internal forces develop between the blocks of permanent magnet assemblies. Large permanent quadrupoles such as Q1 in PEP II are built up from stacks of ring-like slices shown in Fig.15. Internal repulsive forces between slices of Q1 (OD 166 mm ID 87 mm, 1 Tesla Sm_2Co_{17}) are 1.5 tons [7].

6. Detector Solenoid Compensation

The detector solenoid field will have two separate effects on stored beams.

a Vertical and horizontal betatron oscillations will be coupled by the axial field.

b Since it is not possible to align the two separate beam trajectories with the solenoid axis, it will cause orbit shifts. In PEP II, these are held to $\simeq$ 1 mm at the first septum quad by tilting the detector axis to the mean bend angle of the dipole separation magnets.

The traditional method of betatron coupling compensation is to make $\int \mathbf{B} \cdot dz = 0$ through the detector. It is not practical to get large $\int \mathbf{B} \cdot dz$ using permanent magnet solenoids. In the PEP II design, compensation must be done with skew quadrupoles external to the detector. For superconducting final focus designs, strong compensating solenoids are easy to incorporate into the quadrupole cryostat. The magnetic repulsion between this coil and the detector solenoid must be considered in the design of the cryostat support. If the compensator extends from the low field of the detector entrance into the uniform field region, integrating the "magnetic pressure" over the compensator end face of a typical compensator $F = \int \frac{B^2}{2\mu_0} da$ gives:

$$F \simeq \frac{(1.5 \text{ Tesla})^2}{2\mu_0} \pi (.20 \text{ m})^2 = 12.5 \text{ tons}$$

7. Magnet Support Structures

Large heavy magnets will have to be aligned and stably supported inside a B-factory detector. Total IP magnet weight is 1.5 to 3.0 tons. Alignment tolerances are on the order of 100 μm over the 5 m length of the detector. Alignment to this degree is difficult because magnets are not readily surveyable once inside the detector. Mechanical vibration must be limited to $\sim 0.2\mu$ m and longer term thermal drifts to tens of microns. In addition it must be possible to open the detector for servicing. A variety of support approaches have already been tried in earlier detectors:

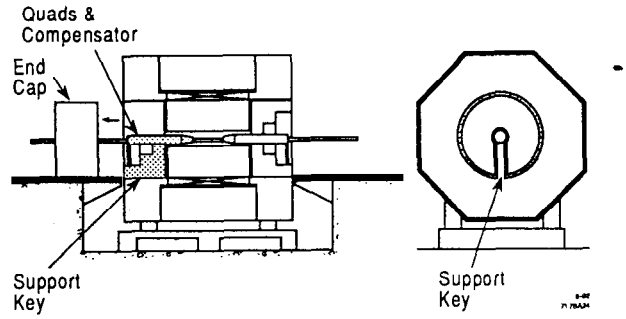

Figure 16. Early SLAC MK II detector(1972) supported the final beamline magnets on a fixed portion of the iron end cap. The remaining instrumented semicircle of the endcap could then roll back along the beamline for access.

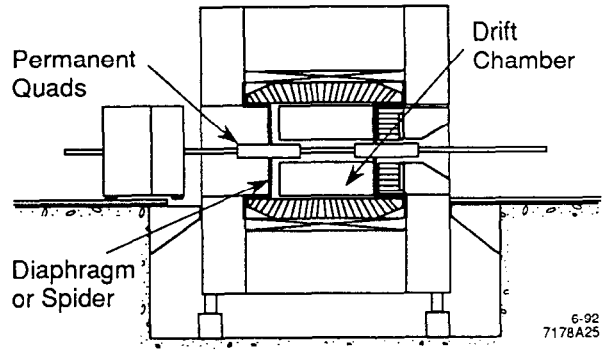

Figure 17. Cornell CLEO Detector uses a diaphragm or spider across the drift chamber end face to support each quad at its balance point.

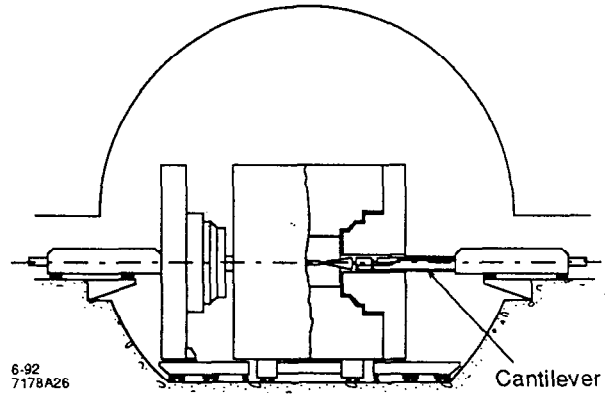

Figure 18. CERN Delphi detector(1983) uses a cradle cantilevered into the detector from each end to support the final magnets from the ends of the machine tunnel.

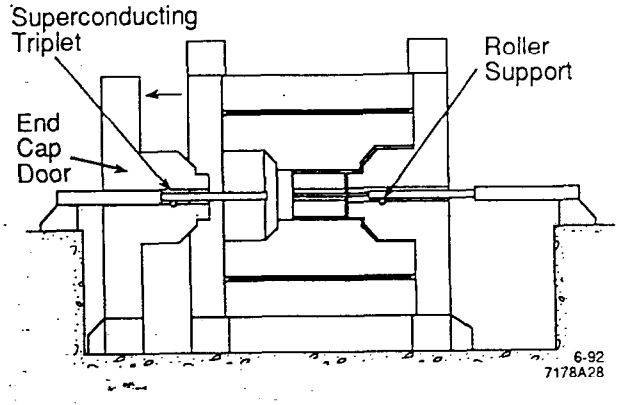

Figure 19. SLAC SLD detector(1986) supports the quadrupoles on a roller at the front end which then rolls back with the endcap door leaving the quadrupole in cantilever support during access.

The support structure proposed for the PEP II B-factory carries the magnets at each end of the detector as well as the central vertex detector all in a common support tube. This weight rests on mounts in the central drift chamber which in turn is supported from the detector coil by a spider structure.

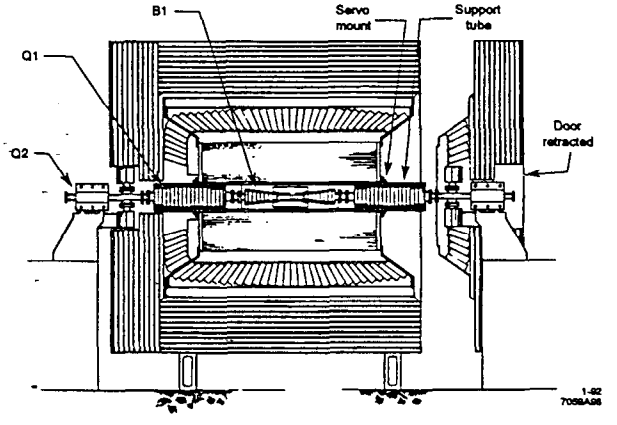

Figure 20. PEP II

This approach makes it possible to assemble and align all of the magnets, masks, and vertex detector into a single structure before it is installed into the detector. Survey and alignment in the lab (fig.21) will allow full view of the structure necessary for 100 μ m alignment. During alignment, support geometry will replicate the as-installed deflections.

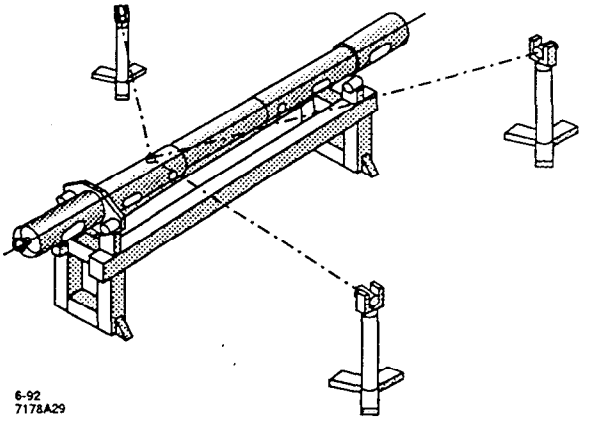

Figure 21. Alignment of Support Barrel

Once installed in the detector, servo positioned kinematic mounts [8] will prevent transmission of distortions through the mounts and also allow small adjustments to barrel alignment during operation. The barrel is assembled with bolts from three separate submodules before internal alignment. Figure 22 shows the right half. Connecting together magnets on both sides of the IP holds them pointed at each other but places additional radiation lengths of material in the track of events. The central section of the support barrel will be made from a sandwich of acrylic foam and carbon fiber skins to minimize radiation length (0.5% X_0) and thermal distortion [9]. In addition to the support barrel material, the inner wall of the drift chamber (1 mm Be) contributes 0.28% X_0 and a He gas cooled double walled Be beam pipe adds another 0.34% X_0. Whether mounting all IP magnets together in a common structure isolated from the detector is worth the increased material thickness depends on the alignment sensitivity of a two ring high luminosity B-factory.

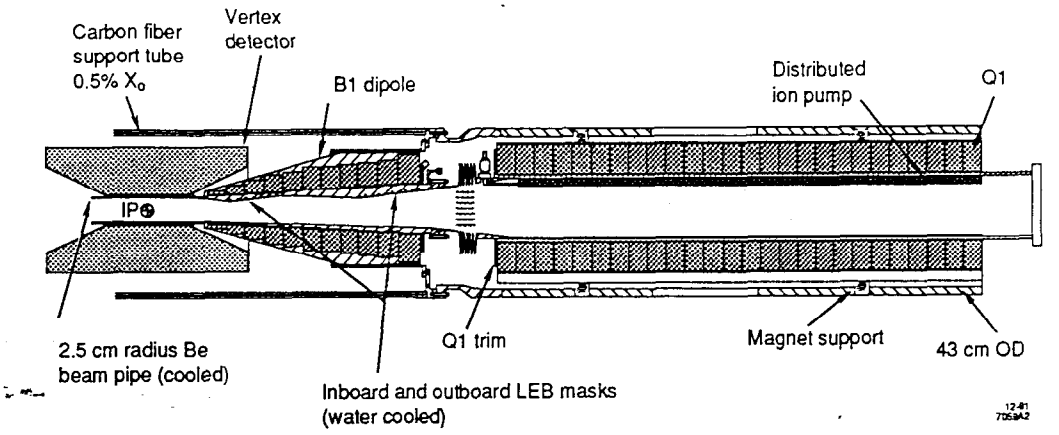

Figure 22. PEP II Barrel Cross Section

REFERENCES

[1] P. Morton,P.Wilson,SLAC AATF/79/15, Nov.1979

[2] S.Heifets, Broad Band Impedance of The B-Factory,SLAC/AP-93, Feb. 1992

[3] J. Welch, A Simple Analytic Est. of the Loss Parameter of a Large Tapered Chamber, Proc. IEEE Particle Accelerator Conf., May 1991, p.792-94,IEEE Press 1991

[4] J.Weaver, P.Wilson, J.Styles, Bench Measurements of the Loss Impedance for PEP Beam Line Components, SLAC-PUB-2284

[5] K.Halbach, Physical and Optical Properties of Rare Earth Cobalt Magnets, NIM 187 (1981), p109-117

[6] S. Kurokawa, KEK Superconducting Quad, these Proceedings

[7] G.Bowden, Magnetic Forces Inside Permanent Magnet Assemblies, SLAC ABC Note 067, March 1992

[8] G.Bowden, Kinematic Cam Positioning Mounts, Workshop on Vibrational Control and Dynamic Alignment Issues at the SSC, SSCL-SR-1185, Feb. 1992

[9] H.Betzold and G.Lippmann, Application of carbon fibre composite materials for collision sections of particle accelerators, Proc. IEEE Particle Accelerator Conf, May 1991, p.792-94,IEEE Press 1991